Maritime Transport Research 5 (2023) 100096

Contents lists available at ScienceDirect

Maritime Transport Research

journal homepage: www.elsevier.com/locate/martra

A high-fidelity approach to modeling weather-dependent fuel consumption on ship routes with speed optimization

Andreas Breivik Ormevik [a,*], Kjetil Fagerholt [a], Frank Meisel [b], Endre Sandvik [c]

[a] Department of Industrial Economics and Technology Management, Norwegian University of Science and Technology, NO-7491 Trondheim, Norway
[b] Institute for Business Management, Kiel University, Kiel 24098, Germany
[c] SINTEF Ocean AS, NO-7052 Trondheim, Norway

ARTICLE INFO

Keywords:
Operations research
Maritime logistics
Weather-dependent vessel routing
Fuel consumption modeling
Speed optimization

ABSTRACT

In this paper, we present the scheduling problem on a given route where speed optimization under various weather conditions is to be performed. Different approaches for calculating fuel consumption for vessels are introduced with a discussion of how this might influence the speed optimization strategies on predetermined multi-stop routes in a short sea shipping service within offshore logistics. Due to both spatial and temporal changes in weather conditions, fuel consumption as a function of speed becomes time-dependent as a vessel performs its route in varying weather. In our novel approach, the weather impact on fuel consumption for the considered vessels is modeled with a higher level of detail than in previously conducted studies, including both wave direction and wave period as input together with the wave height. We test our approach for optimizing schedules on a large set of routes of different lengths and number of stops, as well as for a set of different weather samples based on historical observations. When comparing the new approach to current industry practice, the computational study reveals on average a 4.5% reduction in fuel consumption across the different routes and weather scenarios. The magnitude of the reduction potential increases for worsening weather conditions. Furthermore, it is demonstrated how the approach commonly used for modeling weather impacts in the literature tends to greatly miscalculate the true cost of performing a voyage in realistic weather conditions. Finally, we discuss how the model fidelity is likely to affect the outcome of the routing decisions at a higher planning level, representing a potential for even further reductions of fuel consumption in various weather conditions.

1. Introduction

Operational planning problems within maritime transportation face several practical considerations that are not present in corresponding onshore planning problems. Perhaps the most significant difference relates to the highly weather-dependent performance of ships, as certain weather conditions restrict their operations in terms of capacity, range and attainable sailing speeds. Due to this, an area that recently has seen a considerable growth in interest is the *ship weather routing* problem. In the recent survey of Zis et al. (2020), the ship weather routing problem is defined as determining the optimal sailing path across the sea along a *given* voyage, when also taking into account the expected weather and sea conditions (e.g., from weather forecasts). The problem differs from the well-known *ship routing and scheduling* problem, which focuses on determining the sequence of port calls (or routes) for a

* Corresponding author.
E-mail address: andreas.ormevik@ntnu.no (A.B. Ormevik).

https://doi.org/10.1016/j.martra.2023.100096
Received 8 April 2023; Received in revised form 8 June 2023; Accepted 27 June 2023
Available online 18 July 2023

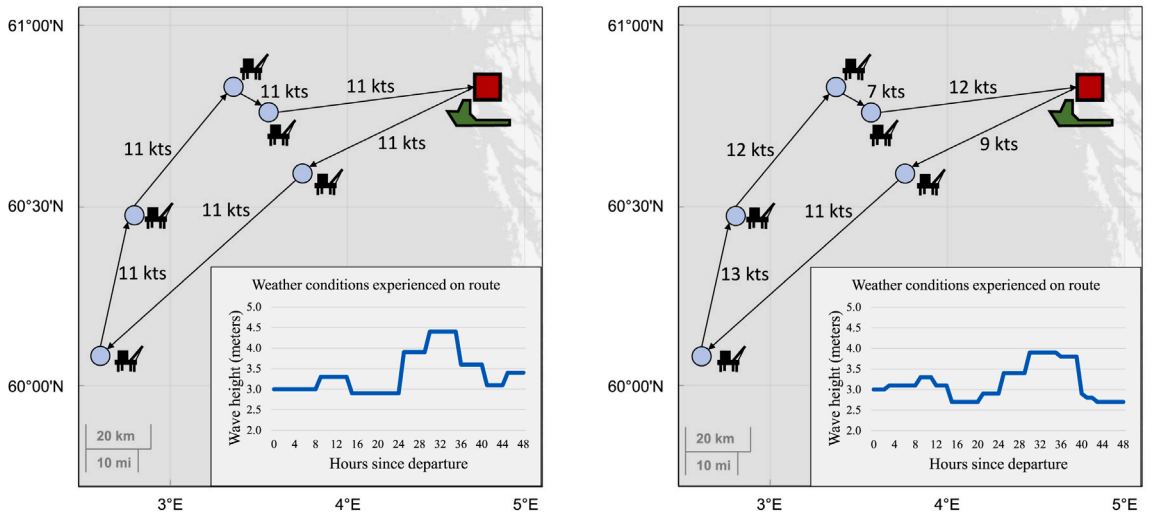

(a) Route planned with constant sailing speed.

(b) Route planned with speed optimization.

Fig. 1. Example of weather-dependent speed optimization on a route that needs to be completed with an average sailing speed of 11 knots. Compared to applying a fixed speed of 11 knots on every sailing leg (left), our novel approach yields adjusted speeds (right) with a 15% lower fuel consumption.

set of vessels (e.g., Christiansen et al. (2013)). Both types of problems can be integrated with a *speed optimization* procedure where setting the sailing speeds along the route becomes a part of the planning. This paper focuses on a particular weather-dependent speed optimization problem arising in the field of offshore logistics planning for the Norwegian oil and gas industry. Currently, there are around 90 manned platforms used for the oil and gas extraction from the reservoirs on the Norwegian continental shelf. Various activities related to drilling, installations of subsea infrastructure and maintenance require big cargo volumes (relative to the available storage capacity at the installations) of a vast span of different equipment and cargo types. All cargo is distributed using specialized platform supply vessels (PSVs), designed to operate in nearly all weather conditions. Logistics planners create periodic (e.g., weekly) routes and schedules for these PSVs which in itself is a complex planning problem with a large span of possible extensions, see for instance Halvorsen-Weare et al. (2012), Shyshou et al. (2012), or Kisialiou et al. (2018). Next to this, offshore oil and gas production often generates urgent needs for specialized equipment or requires sudden changes to initial activity schedules, which can lead to last-minute changes of cargo demands at installations. Thus, the routing procedure might need to be repeated in order to make adjustments to the routes and schedules of PSVs. During this routing process there is a need for evaluating the cost- or fuel-optimal way of performing the proposed route alternatives, e.g., Ulsrud et al. (2022) and Cuesta et al. (2017). This results in a separate *subproblem* of determining optimal sailing speeds for every leg along a given route. Due to the potential rapid changes in weather conditions for vessels operating along the Norwegian coast, this speed optimization problem becomes time-dependent as sailing at a certain speed at different times might yield different fuel consumption rates. In other words, the fuel consumption curves for the PSVs are dependent on the weather conditions. In this paper, we consider this weather-dependency as an integrated part of the speed optimization problem.

To highlight some key features of the weather-dependent speed optimization within offshore logistics, we consider the following example: Five installations are to be visited by a PSV in a given sequence, and the route needs be completed within 48 h. Based on the geographical distances and the service times at the installations, the PSV needs to maintain an average speed of 11 knots throughout the route in order to complete the route on time. Without speed optimization, all legs along the route would be traveled at constant speed of 11 knots, as illustrated in Fig. 1(a). The figure also illustrates the time-dependent weather conditions in terms of wave heights that the PSV faces along its route under this fixed speed. Fig. 1(b) shows the adjusted speeds that we obtain from the modeling approach that is introduced in this paper. In this approach, we consider weather not just in terms of wave heights but also direction and periods of the waves. As can be seen in the figure, this optimized speed regime limits the magnitude of wave heights experienced along the route, where the maximum wave height never exceeds 4.0 m. This results in a reduction of fuel consumption by 15%, corresponding to approximately four tons of CO_2.

The main purpose of this paper is to evaluate how the precision level of modeling weather impact affects the sailing speed decisions for a given PSV route. Halvorsen-Weare and Fagerholt (2011) discuss how the significant wave height is the single most influential factor that affects both sailing speed and servicing times at installations for the PSVs. They provide a simplified discrete impact matrix for different weather states defined by the significant wave height (H_s), see Table 1. Dependent on the current significant wave height, a certain reduction Δv to the maximum attainable speed is experienced by the vessels. Furthermore, the overall time and fuel consumption required to service the offshore installations with their requested demands increase by ΔT^S and Δf^S percentage points, respectively. Note that, according to Table 1, the PSVs will have to "wait on weather" and have forced idling before service can take place at an installation if the significant wave height is more than 4.5 m.

Table 1
Four weather states (WS) based on significant wave heights (H_s) and the impact on the PSVs in terms of enforced reduction of maximum attainable speed (Δv), as well as relative increases of required time ($\Delta T^{\cdot S}$) and fuel consumption ($\Delta f^{\cdot S}$) for servicing offshore installations.

WS	H_s (m)	Δv	$\Delta T^{\cdot S}$	$\Delta f^{\cdot S}$
0	≤ 2.5	0	0	0
1	(2.5, 3.5]	0	20%	20%
2	(3.5, 4.5]	−2 knots	30%	30%
3	> 4.5	−3 knots	*Forced idling*	100%

While the implementation of this approach is relatively straightforward, it represents a strong simplification of the real weather impact on operating a PSV. Numerical methods exist for better approximating weather impact, and simulation-based software tools can provide deeper insights to the real impact of various weather conditions to ship performance in an operational setting. As discussed by Norlund and Gribkovskaia (2017), this could by beneficial in the planning of PSV operations for offshore logistics which often takes place in extreme weather conditions. However, no studies exist so far that actually consider this. To close this gap, our paper aims at answering two key research questions regarding the operational planning of offshore logistics and similar short sea shipping services subject to varying weather conditions:

1. To what extent are the obtained sailing speeds along given routes affected by the fidelity (resolution) of weather-dependent models for calculating fuel consumption?
2. In a broader context with multiple vessels and customers/ports to service, will also the routing strategy (i.e., the construction of optimal routes) be altered by the choice of model fidelity?

The remaining parts of this paper are structured as follows: Section 2 provides a more thorough description of existing research on the field of weather-dependent maritime routing problems, with a particular focus on offshore logistics. In Section 3, the considered shipping service under consideration is described, followed by a formulation of the speed optimization problem and a description of the proposed solution approach with discretized arrival times. In Section 4, the high-fidelity model used to represent weather impact in a more precise manner is described, along with a discussion of practical aspects affecting the fuel consumption curve for the PSVs considered in this paper. Section 5 contains the computational study, where a comparison of different approaches to model weather impact is made. Section 6 concludes the conducted work.

2. Literature review

This section presents a selection of relevant literature regarding the two main features of our considered planning problem, namely weather routing and speed optimization.

Weather routing

Simonsen et al. (2015) point out the main components required in a weather routing model, namely a fuel consumption model for the vessel under consideration, a weather forecast for the geographical area of interest, and an understanding of the vessel's response to the weather conditions encountered during the voyage. The survey conducted by Zis et al. (2020) provides an overview of the growing interest within the field of weather routing, with approximately 50 new papers published annually since 2015. Their survey presents weather routing problems with a large span of optimization objectives not limited solely to minimizing fuel consumption. Due to safety concerns, avoiding severe storms or sea ice can be paramount for the routing process and hence favor sailing options with a lower risk level, but higher fuel consumption.

Walther et al. (2016) discuss key aspects of modeling and solving weather routing problems. The majority of the conducted research is focused on modeling approaches involving a discretization of time or space to avoid non-linear model formulations. Dynamic programming and genetic algorithms are frequently applied, but also variants of the isochrone method as first introduced by James (1957) are discussed. The first weather routing models assumed fixed sailing speeds for all parts of routes even for applications within deep sea shipping. In recent years, the weather routing problems are enriched with features including multi-objective optimization and information about sailing speed (sailing time), and such complex weather routing problems can be solved e.g., by the implementation of bio-inspired algorithms. Zhang et al. (2021) use an ant colony optimization algorithm to solve a multi-objective weather routing problem where navigation safety and sailing time are objectives in addition to minimizing the fuel consumption. Du et al. (2022) solve a weather routing problem with engine power (speed) as a decision variable, and propose a variant of the practical swarm optimization algorithm to solve the problem. The solution approach that we propose in this paper is based on Dijkstra's algorithm, another frequently applied solution method for weather routing problems.

The majority of the relevant studies on weather routing applies to the deep sea shipping segment, i.e., the intercontinental trade over long distances. For such routing problems, several significantly different sailing path options exist. The least fuel-consuming geographical path for the oceanic crossing will heavily depend on the spatial and temporal variation of large weather systems encountered during the voyage.

One general challenge with weather routing in deep sea shipping relates to numerical uncertainties of the weather routing model resolution which, as described by Dickson et al. (2019), can be as high as 125 km (spatial) and three hours (temporal) when retrieving

weather data from standard climate models. They further discuss how finer node resolution (smaller distance between geographical grid points) greatly influences the selected optimal paths for given routes, and hence also the weather conditions experienced by the vessel under consideration. Another source of uncertainty relates to the weather forecasts, which can be quite inaccurate for later stages of long-haul routes. Mason et al. (2023) address the challenge of uncertainty in wind forecasts for ships with wind-assisted propulsion, and show how this greatly affects the theoretical fuel saving potential when realizing routes based on the a priori routing decisions. To limit the losses in the fuel saving potential, they suggest an adaptive optimization strategy where forecast data are updated every 12 h and routing decisions are adjusted accordingly.

Offshore logistics, on the other hand, can be categorized as a typical example of *short sea* shipping, defined by Paixão and Marlow (2002) as maritime transportation over relatively short distances. There are certain features of such shipping services that make the associated weather routing problems and hence the modeling approaches different from the ones applicable for deep sea shipping. The planning period is usually limited to a couple of days, and, hence, one can consider weather forecasts to be relatively accurate. As discussed by both Zis et al. (2020) and Simonsen et al. (2015), this allows for a more detailed assessment of weather impact to the vessels in operation.

Kepaptsoglou et al. (2015) consider wind and wave impact for short sea shipping services in the Aegean Sea, and formulate a chance-constrained model for a vessel routing problem with stochastic travel times due to weather impact. The problem is solved using a genetic algorithm. Sen and Padhy (2015) present an approach for developing a ship routing algorithm based on detailed empirical hydrodynamic models for calculating weather impact to vessel operability. They apply the approach on a coastal shipping route in the North Indian Ocean region. The economic benefits of weather routing for short sea shipping services in the Mediterranean are investigated by Grifoll et al. (2018), who reports up to 18% cost savings during periods of bad weather. Their weather impact model is based on a simplified empirical expression for the speed losses induced by waves of certain heights and from certain directions. The same approach to model weather impact is taken by Grifoll et al. (2022), who present the application of a free software for ship weather routing based on the A* pathfinding algorithm. They test the software on different short sea shipping routes across the European continent in addition to transatlantic routes, and report how the optimal routes have longer distances that can be covered with a lower fuel consumption in less time, due to smaller speed losses induced by the weather conditions.

It should be noted that all conducted research mentioned above involves determining sailing paths across the sea. For the case of offshore logistics, sailing legs are in general too short for allowing alternative sailing paths between installations. This implies that bad weather usually cannot be fully avoided through "detouring". Therefore, in our paper, we consider the route and the sailing path along the route to be completely fixed. Weather "routing" can in this study therefore be understood as a speed optimization problem aiming to limit the share of the route duration spent on sailing in bad weather.

Speed optimization

The selected sailing speed has a significant impact on the fuel consumption of most vessels. Therefore, extensive research has been conducted addressing speed optimization within maritime transportation. Psaraftis and Kontovas (2013) discuss how so-called "slow steaming" to various extents has been used by shipping companies with significant reductions in fuel consumption and CO_2 emissions. However, slow steaming is not necessarily equal to optimizing speed in maritime applications. As a response to the lack of a clear definition of the term "speed optimization" in regulatory documents by the International Maritime Organization (IMO), Psaraftis (2019) defines speed optimization as "the selection of an appropriate speed profile" to achieve a particular objective (such as fuel costs or emissions) subject to a set of various operational constraints. From this definition, also higher sailing speeds for specific legs on a route can yield the overall optimal solution, if this in turn reduces costs or emissions on other parts of the voyage.

In the extensive survey on speed models and the proposed taxonomy for energy-efficient maritime transportation, Psaraftis and Kontovas (2013) present an overview of the main influential factors affecting optimal vessel sailing speeds, such as the payload level, fuel price, state of the market and weather conditions. They also distinguish between whether speed optimization is applied to a set of fixed shipping routes, or if it is an integrated part of a ship routing and scheduling problem. The planning problem considered in this paper belongs to the former category, where routes have been determined prior to the speed optimization procedure.

Norstad et al. (2011) consider an integrated tramp ship routing and speed optimization problem, where the routing decisions are affected by the selected sailing speeds and corresponding fuel consumption. Evaluating the performance of a route option depends on the speed-optimized schedule for the route, and this separate, non-linear speed optimization problem was formally introduced by Fagerholt et al. (2010). They discuss a set of solution approaches to the speed-optimization problem on given ship routes, which we further elaborate on in Section 3.

Eide et al. (2020) consider load-dependent speed optimization in a maritime inventory routing problem, i.e., where the fuel consumption is calculated based on both the selected sailing speeds and the loading condition of the vessel at the time of sailing. They propose an arc-flow model for the problem which is solved by linearizing the convex fuel consumption curves for each loading state. They report large savings from the speed optimization when considering the load at the time of sailing each leg on each route. Research on speed optimization in maritime applications also involves several other practical aspects of the shipping services under consideration. Yang et al. (2020) develop a model taking into account the ocean currents to calculate the correct speed of the vessels (relative to the water), which clearly has an impact on the calculated fuel consumption rate in various weather conditions and sailing speeds. Regarding the weather impact to the operability of vessels, Li et al. (2020) study how *voluntary* speed losses (i.e., deciding to reduce the sailing speed) in speed optimization models create schedules with different sailing speed profiles and lower overall fuel consumption, compared to instances where speed reductions are forced (i.e., involuntarily) due to physical limitations of the vessel's operability in harsh weather conditions.

With respect to speed optimization in offshore logistics planning, Norlund and Gribkovskaia (2013) address the effects of including speed optimization in tactical supply vessel planning, i.e., when creating weekly schedules for a fleet of PSVs operating in the North Sea. They apply a cubic relationship, $\left(\frac{v}{v_0}\right)^3$, to calculate the scaling factor for fuel consumption when sailing in speed v relative to the design speed v_0 on a leg of a proposed route. For experiments carried out using real data, they report potential fuel cost (and hence emission) reductions of 25% without the need of increasing the fleet size. However, they do not consider how weather conditions impact the optimal sailing speeds.

As discussed in Section 1, Halvorsen-Weare and Fagerholt (2011) take weather into account by considering forced speed losses due to wave heights within certain discrete intervals (referred to as *weather states*). Based on this approach, Norlund and Gribkovskaia (2017) extend their previously mentioned work and modify the cubic fuel consumption by also including this fixed speed loss associated with a set of discrete weather states in the scheduling of PSVs. They report a large potential for fuel cost savings, but find that the savings from (forced) speed reductions when including the weather considerations might be restrained by the need for adding extra vessels to the fleet and hence pay additional charter costs.

Ulsrud et al. (2022) are the first to integrate the weather impact modeling approach of Halvorsen-Weare and Fagerholt (2011) into an operational routing problem for offshore logistics. They consider the routing of a fleet of PSVs such that the orders placed by offshore installations shortly before departure can be met in a cost-optimal way, either by the controlled fleet or by short-term chartering of external spot vessels. A small set of different fictive weather samples are created to highlight the importance of accounting for weather impact in the routing. They report a potential of fuel savings of approximately 20% compared to applying a fixed speed, which is in accordance with the findings of Norlund and Gribkovskaia (2017).

While these studies involve routing of vessels as well as speed optimization on the selected routes, our study considers the speed-optimization on a given route. This allows for a more thorough elaboration on the different weather impact modeling approaches and how these affect the potential for fuel savings when performing the routes under real weather conditions.

3. The weather-dependent speed optimization problem

Section 3.1 provides a definition, including a mathematical formulation, of the weather-dependent speed optimization problem considered in this paper, while Section 3.2 gives an overview of the proposed solution approach.

3.1. Problem definition

We consider a given route that is to be sailed by a PSV over the next few days. As input beside the route, we also have a weather forecast for the relevant geographical region. Since the maximum duration of the route typically is two or three days, this weather forecast is normally very precise. Hence, we consider this weather forecast as deterministic and as a true representation of the weather the PSV will face while sailing this route. Furthermore, this also means that we assume that we know the time windows in which the weather is so bad at the different installations that the PSV will have to "wait on weather" (as explained in Section 1).

We define the considered *route* as a sequence of sailing *legs* between offshore installations (or ports) modeled as *sequenced nodes* along the route in the set $\mathcal{N}$, indexed by i. For a given route starting from the supply depot in node 0 and with n further installations (or ports) to visit, the sequence of node visits is given as $0, 1, 2, \dots, i, (i+1), \dots, (n-1), n$. In the context of offshore logistics, the route is a round-trip, such that node n represents the return to the supply depot. The route has a maximum allowed duration T^{MAX} (typically two or three days) specifying the latest possible arrival time at node n. The sailing legs (n in total) are denoted $(i, i+1), i \in \mathcal{N} \setminus \{n\}$, each with a given distance of $D_{i,i+1}$. We distinguish between three time variables in this model: The arrival time at an installation i is denoted t_i^A. In cases of arrival outside the time window specified as $\left[\underline{T}_i, \overline{T}_i\right]$, which is dependent on both opening hours at the installations and periods of severe weather conditions, idling is required for the PSV until servicing can start at time t_i^S. The service time, $S_i\left(t_i^S\right)$, required to complete service at an installation i, is calculated as a function of the start time for the service. In other words, the service time is weather-dependent as the varying weather conditions affect the ability to perform cargo handling. Finally, the third time variable t_i^D defines the time of departure from installation i, which takes place immediately after completing the cargo handling operations.

We assume that the energy (fuel) consumption is known for a certain speed and weather condition. Since the weather conditions will vary over time, we can, for every sailing leg $(i, i+1)$, define a function for the energy (fuel) consumption rate per distance unit, $C\left(v_{i,i+1}, t_i^D\right)$, depending both on the chosen sailing speed $v_{i,i+1}$ and time of departure t_i^D. This function is defined over an interval of feasible sailing speeds, which again is time-dependent since the weather conditions affect the vessel operability and maximum sailing speed. We thus denote the feasible sailing speed interval on leg $i, i+1$ when departing from installation i at time t_i^D as $\left[\underline{V}\left(t_i^D\right), \overline{V}\left(t_i^D\right)\right]$. Furthermore, the total energy (fuel) consumption during cargo handling operations at installation i is dependent on the weather conditions at the time of servicing, and is hence denoted $C_i^H\left(t_i^S\right)$. Finally, the total energy (fuel) consumption during idling due to bad weather or arrival outside the opening hours at the installation, depends on the arrival time t_i^A and is defined as $C_i^I(t_i^A)$. Note that in cases where servicing can commence immediately after arrival (i.e., when $t_i^S = t_i^A$), the idling consumption will be zero.

From this we can formulate our speed optimization problem as follows:

$$min \sum_{i=0}^{n-1} \left[D_{i,i+1} C\left(v_{i,i+1}, t_i^D\right) + C^H\left(t_{i+1}^S\right) + C_{i+1}^I\left(t_{i+1}^A\right)\right], \tag{1}$$

subject to

$$t_i^D = t_i^S + S_i\left(t_i^S\right), \quad i \in \mathcal{N} \setminus \{0\}, \tag{2}$$

$$t_0^D = 0, \tag{3}$$

$$t_{i+1}^A = t_i^D + D_{i,i+1}/v_{i,i+1}, \quad i \in \mathcal{N} \setminus \{n\}, \tag{4}$$

$$t_i^S = max\left\{t_i^A, \underline{T}_i\right\}, \quad i \in \mathcal{N} \setminus \{0\}, \tag{5}$$

$$\underline{T}_i \le t_i^S \le \overline{T}_i, \quad i \in \mathcal{N} \setminus \{0, n\}, \tag{6}$$

$$t_n^D \le T^{MAX}, \tag{7}$$

$$\underline{V}\left(t_i^D\right) \le v_{i,i+1} \le \overline{V}\left(t_i^D\right), \quad i \in \mathcal{N} \setminus \{n\}. \tag{8}$$

The objective function (1) minimizes the overall fuel consumption for the route as a sum of transit consumption for all sailing legs along the route, consumption during cargo handling at every installation, and the idling consumption when required due to the time of arrival. Constraints (2) set the departure time equal to the time of service completion at every installation, and the initial departure time from the origin (where no service is performed) is controlled by Constraint (3). The arrival times are calculated from Constraints (4). As seen from Constraints (5), servicing each installation can at earliest commence at the start of the specified time window, or at the actual arrival time if this is within the time window. Constraints (6) make sure that all installations are serviced within their time windows, and Constraint (7) ensures that the vessel ends the route within the specified maximum duration. Constraints (8) keep the selected sailing speeds within the time-dependent speed interval on all legs.

3.2. Solution approach

The above formulation extends the one by Norstad et al. (2011), where the speed optimization problem arises as a subproblem to the routing in a real-life tramp shipping service. They propose a recursive smoothing algorithm for solving this non-linear problem, where the idea is that the convexity of the fuel consumption function makes it optimal to keep the average speed as close to the most fuel-efficient speed as possible for as much of the sailed voyage as possible. In other words, sailing two route legs of equal length at 16 knots will always be better than sailing the two legs at 14 and 18 knots, respectively, unless time windows require speed-up at certain legs. However, as clearly stated by the authors, this recursive smoothing algorithm can only be applied in cases where the fuel consumption function is convex and remains the same throughout the entire route. This requires the consumption to be independent of the onboard load or weather conditions, as sailing in 14 knots fully loaded (or in harsh weather) actually can be more fuel consuming than sailing 18 knots without cargo (or in calm weather). When weather is assumed to affect the fuel consumption on a leg, the authors suggest to apply a shortest path solution approach first introduced by Fagerholt (2001), where the arrival times to each stop along the route are discretized based on feasible speed alternatives. A directed, acyclic graph can then be created on a time–space diagram and solved as a shortest path problem.

The described approach is well suited for handling the weather-dependency of the considered speed optimization problem in this paper. As it is assumed that no idling can take place after completing service at an installation such that the vessel departs immediately, we define in our time–space diagram a node (i, p) for every discrete departure time p. This means that an arc $((i, p), (i{+}1, p'))$ in the time–space diagram contains information about all vessel activities associated with a sailing leg: After departing installation i at the discrete time point p, transit sailing to installation $i + 1$ is performed where servicing and potential idling is performed before the next departure takes place at time p'. The feasible speed interval for performing sailing, $\left[\overline{V}(i, p), \underline{V}(i, p)\right]$, is dependent on the departure time which specifies the current weather conditions. From this speed interval, a set of feasible discrete arrival times at installation $i + 1$ can be defined, which in turn gives the weather-dependent servicing time and consumption at the installation. In cases where an arrival time point is outside the specified time window at the installation, weather-dependent idling time and consumption is also calculated and included in the overall energy (fuel) consumption on the arc, $C_{((i,p),(i+1,p'))}$.

Fig. 2 illustrates a time–space diagram with discretized times where the range of feasible sailing speeds for each sailing leg is given such that only nodes (i, p) involving feasible sailing speeds are included in the graph. As stated, arcs are defined to include both sailing, idling and servicing, and as no idling is allowed after servicing an installation the arcs connect the feasible discrete *departure* times at every installation on the route. As can be seen in the figure, two feasible options exist for reaching installation $i{+}1$ from the origin node and completing service at the same discrete time point, p'. The calculated overall fuel consumption, however, can be different as the sailing and servicing might be performed in different weather conditions on the two sailing legs. To find the schedule for the route minimizing the overall fuel consumption, a shortest path problem is solved (e.g., using Dijkstra's algorithm) based on the feasible arcs created in the directed, acyclic graph.

Our mathematical model formulation contains sailing *speed* as the only decision variable, while in our solution approach, the optimal solution is found as the shortest path in a network of arcs represented by points in *time* for departure and arrival. To clarify how sailing speed and time relate in our solution approach, consider the following numerical example illustrated in Fig. 3. Here,

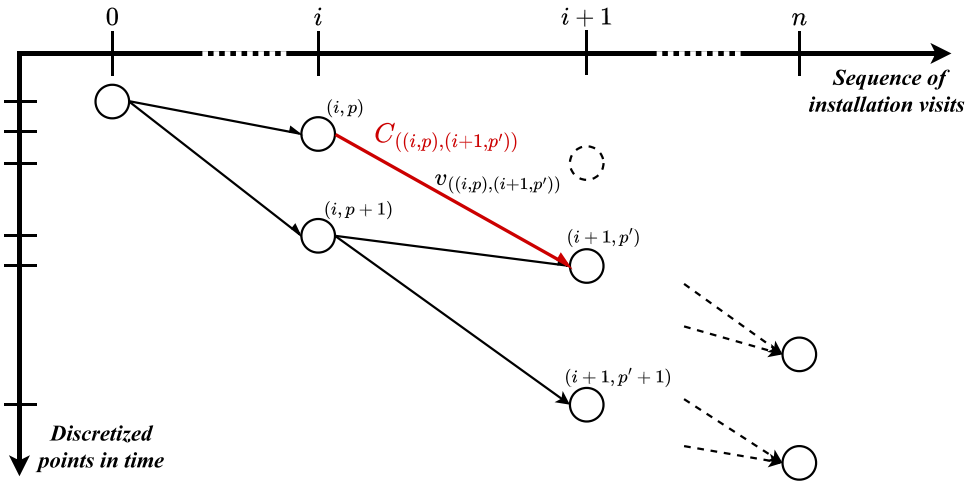

Fig. 2. A time–space diagram for the speed optimization problem on a ship route using discretized times. On the arc $((i,p),(i+1,p'))$, the vessel departs installation i at time p and sail towards installation $i+1$ at speed $v_{((i,p),(i+1,p'))}$, where servicing and potential idling takes place and is completed at time p'. The total fuel consumption for all activities included in an arc is calculated and denoted $C_{((i,p),(i+1,p'))}$. Arcs with sailing speeds outside the feasible speed interval $\left[\overline{V}(i,p), \underline{V}(i,p)\right]$ are disregarded.

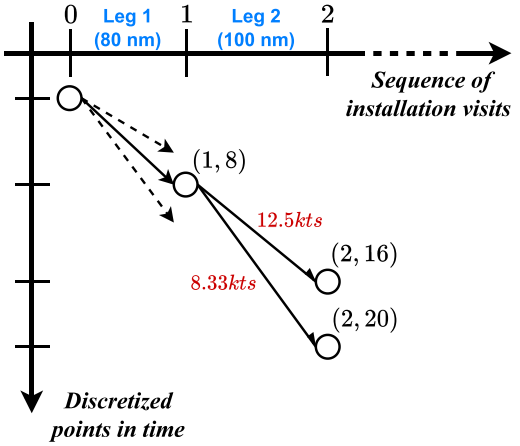

(a) A small example of how the sailing options on each leg are enumerated using discretized time.

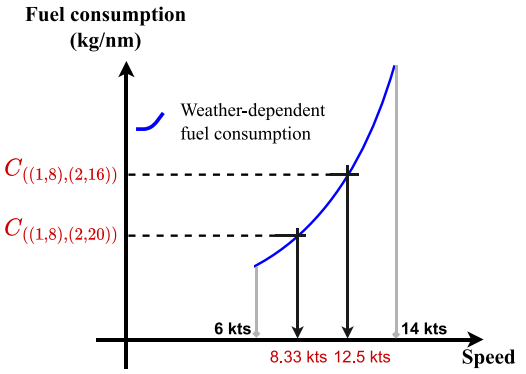

(b) Weather-dependent fuel consumption rates (kg/nm) as a function of speed for a given sea state.

Fig. 3. A simplified arc network using discretized time for departures and arrivals (a) with sailing speeds implicitly given from the route duration (and distance), which translate to arc fuel consumptions from considering the weather-dependent consumption rates in the current weather conditions (b).

we assume a route where the second leg (from installation 1 to 2) has a distance of 100 nm and where we now evaluate the sailing options departing from installation 1 at time period 8 (i.e., eight hours since the departure from the depot, installation 0). Due to weather conditions, we assume that the range of feasible arrival times to installation 2 spans from points in time corresponding to 16 to 20 h after the beginning of the route (yielding a leg duration between eight and 12 h). Based on the time discretization factor, all possible arcs with arrival times representing a leg duration between eight and 12 h are then generated, although we in Fig. 3(a) only illustrate the two arcs corresponding two sailing speeds of 12.5 and 8.33 knots, respectively. Based on the current weather conditions at departure from installation 1, we know the weather-dependent fuel consumption rate as a function of sailing speed as presented in Fig. 3(b). To calculate the fuel consumption along the two arcs $((1,8),(2,16))$ and $((1,8),(2,20))$, consumption rates are simply read from the consumption curve. The calculated arc costs are then stored and used for solving the shortest path problem through the full network to find optimal schedules for the route.

It should be noted that we assume for this paper that the sailing speed remains constant over an entire sailing leg. This is in accordance with the previously conducted studies that used other approaches for modeling weather impact on which we base our comparisons in Section 5. However, the presented model formulation and solution methodology allow for extending this by partitioning each sailing leg into shorter *sublegs* with no time windows and no cargo demand (and hence zero servicing time).

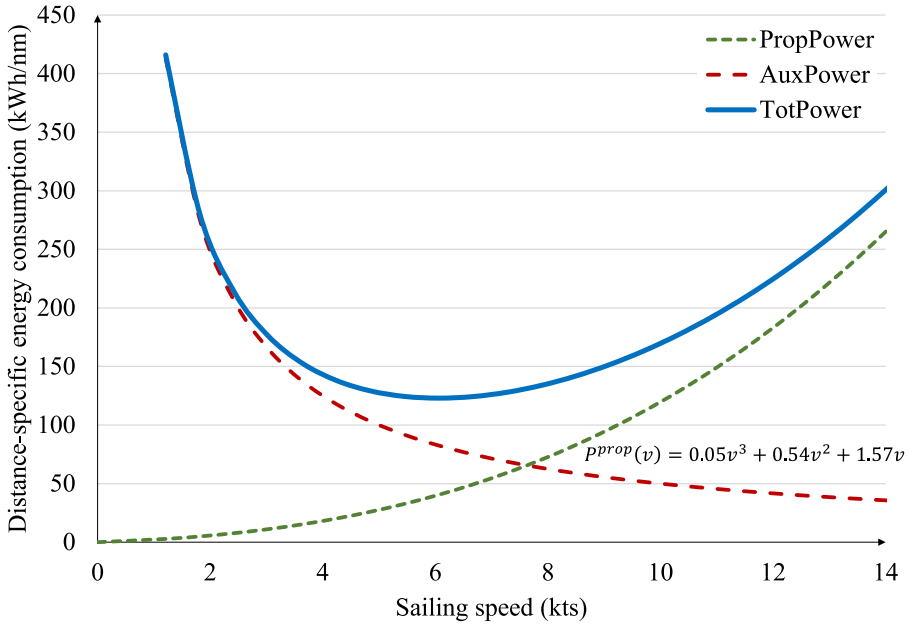

Fig. 4. The approximated convex, distance-specific energy consumption rate in calm seas (i.e., without weather impacts) for the platform supply vessels under consideration. The overall power requirement is the sum of propulsion and auxiliary power requirements.

4. Establishing a high-fidelity fuel consumption model

This section elaborates on the main elements of fuel consumption for vessels, and how weather impacts the relationship between sailing speed and consumption. The modeling approach discussed in Section 3 using discretized arrival times is applicable for all types of fuel consumption calculations, as they just represent alternative procedures for quantifying the consumption parameter $C_{((i,p),(i+1,p'))}$ from Fig. 2. However, different calculation methods might affect the ranking of different speed options in terms of cost (or consumption), and hence the cheapest (or least consuming) path selected in the time–space diagram when solving the speed optimization problem. In the following, some key technical aspects are presented regarding ship operability and hydrodynamics, along with a brief description of the numerical tool used to establish our high-fidelity fuel consumption model.

4.1. Basic fuel consumption theory

Fuel consumption per time unit (e.g., kg/hr) has often been assumed to be cubic related to the sailing speed. To establish an estimate for the fuel consumption, information about both the specific fuel consumption (typically given in g/kWh) and the power requirement (given in kW) is needed. The overall power requirement consists of two main terms described in the following.

The *propulsion* power relates to the forces needed to move a vessel through water at a desired speed. Adland et al. (2020) express the propulsion power as the sum of power components arising from calm water resistance and added resistance due to waves and wind, accounted for efficiency losses. They find that the elasticity of consumption per speed unit is dependent on speed itself, hence the cubic relationship does only hold for speeds near the design speed and they point out the importance of *accurate data-driven estimates of the speed-consumption relationship* for optimization of vessel operations.

In addition to propulsion power, the installed machinery is also used to run any *auxiliary* systems on board the vessel, such as cooling systems, ballast water pumps, air ventilation and electricity to all parts of the vessel. Usually, these power requirements can be considered as constant over time, i.e., independent of the sailing speed. However, it can still be translated into a distance-specific energy consumption given in units of kWh consumed per nautical mile (nm), by dividing the constant load by the sailing speed. The sum of propulsion and auxiliary power gives the resulting total power requirement, and these three are plotted as distance-specific energy consumption curves for the PSV under consideration in Fig. 4.

The PSVs considered in this study have multiple (up to four) main engines installed, where regular operation usually requires only operation on some of the engines (typically two). Above certain threshold values, the power requirement becomes too large for being provided by the current number of operating engines and hence, one additional engine must be used. This in turn requires each engine to operate at a lower average continuous load and with a higher specific fuel consumption. In the computational experiments presented in Section 5, we account for such variations of the specific fuel consumption dependent on the required amount of propulsion power. To the best of our knowledge, this feature has not been considered in previously conducted research.

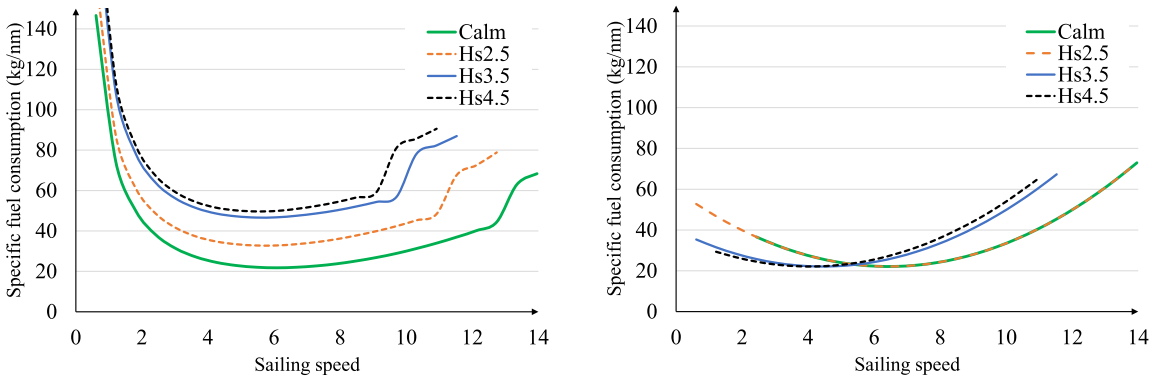

(a) High-fidelity fuel consumption curves, obtained using our novel approach to model weather impact.

(b) Discrete fuel consumption curves, obtained by applying the weather impact modeling from Table 1.

Fig. 5. Distance-specific fuel consumption rates at different sailing speeds in different discrete sea states (assuming only head seas) at two different model fidelity levels. H_s refers to significant wave heights, and sailing speed is given in knots.

4.2. The high-fidelity weather impact approach

There are numerous ways of estimating the weather-induced added resistance to the propulsion power. The numerical hydrodynamic model used to evaluate weather impact in this paper has been constructed using the *ShipX* software developed by SINTEF (2023), combined with in-service data. The modeling approach builds upon the *strip theory* method developed by Salvesen et al. (1970) that is implemented into the program. A calm water performance model, consisting of resistance curves, open water propeller characteristics and propulsion coefficients, is created from the SINTEF Ocean in-house database of experimental results. To calculate the added resistance (and hence increased fuel consumption) induced by different wave conditions, numerical strip theory of the ship hull is used to predict the ship motion characteristics. Furthermore, wind resistance coefficients obtained from Brix (1987) representing typical values for offshore service vessels are used to account also for wind impact. The reader is referred to Kim et al. (2017) for a more thorough description of the theoretical foundation for the modeling approach. Combining these data with a JONSWAP (The Joint North Sea Wave Project) wave spectrum allows prediction of short-term statistical responses, e.g., expected levels of resistance and motions, of the ship during transit in wave and wind conditions. Next, tuning of the model is performed using one week of in-service empirical data from a PSV operating in the North Sea. Lastly, combined with hindcast sea state and wind data from the Norwegian Meteorological Institute, the observed differences in propeller power from the data set and the calm water power model is used to tune the wave added resistance coefficients in low to moderate sea states. The resulting model predicts the expected average propulsion power as a function of ship speed, significant wave height, spectral peak period and wave direction relative to vessel heading. The so-called involuntary speed losses, i.e., the reduction of maximum attainable speed due to insufficient engine capacity in rough weather conditions, can then be calculated. Note that we do not consider voluntary speed losses in our experiments, e.g., decisions on reducing speed due to excessive ship motions or comfort criteria.

The resulting fuel consumption curves for PSVs operating in the North Sea

For conventional PSVs in the North Sea operating on marine diesel oil (MDO), a typical machinery layout would consist of four main engines and a total installed power of approximately 4500 kW. As briefly discussed above, the specific fuel consumption will be based on the number of engines needed to produce the necessary amount of power. Fig. 5(a) shows how the fuel consumption varies for the four different sea states presented in Table 1, assuming wave height as the only parameter influencing the consumption and operability. The sudden "jumps" in fuel consumption displayed in Fig. 5(a) represent the threshold where one additional engine is needed to provide sufficient amounts of power. Furthermore, the upper bound of the fuel consumption curves represents the maximum attainable speed for the different sea states (wave heights). For comparison, the resulting consumption curves obtained when considering weather impact in the more simplified manner are illustrated in Fig. 5(b). As presented in Table 1, wave heights up to 2.5 meters are assumed to affect only the required time and consumption for servicing, and hence the fuel consumption curves in this approach are assumed to be identical for the calm water state and for wave heights of 2.5 m.

Considering only wave heights when evaluating the weather impact on the operation of PSVs clearly simplifies the estimation of the true weather impact and is expected to have an effect on the speed selection and routing decisions within offshore logistics planning. Our high-fidelity model allows a significantly richer evaluation of a larger span of different weather conditions. More specifically, the impact for the four different discrete wave heights presented in Table 1 can be evaluated for a discrete set of relative wave *headings* (compared to the heading of the PSV), and the required power propulsion is provided by the model. From this, isoquant curves can be drawn as shown in Fig. 6, visualizing the maximum attainable speed (i.e., the highest speed that can be achieved given the amount of installed power on board the vessel) for the same four discrete wave heights approaching the vessel from all possible directions. It can be observed that head seas has the largest impact and also yields the largest variation between

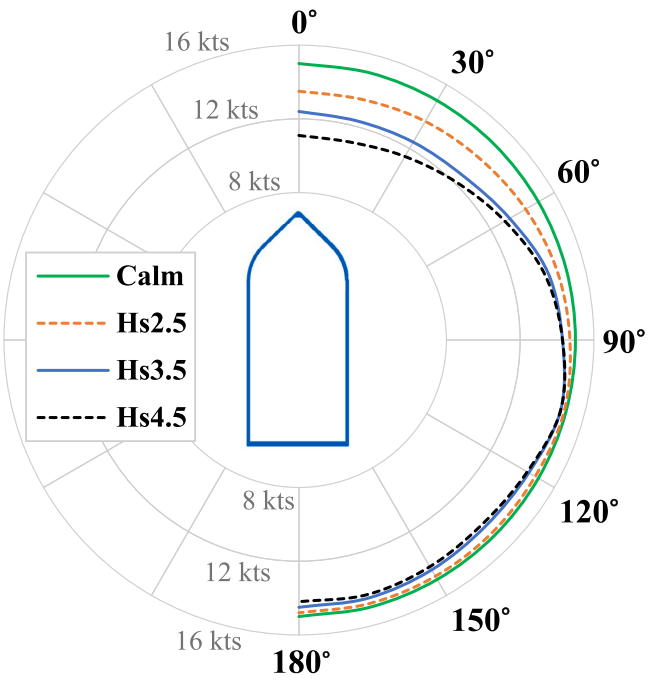

Fig. 6. Dependency on relative heading of waves to the maximum attainable speed for a PSV with a maximum sailing speed of 15 knots in calm water, in the same sea states as presented in Table 1.

the four discrete wave states, while the estimated forced speed reduction is significantly lower for all waves approaching the vessel from behind.

In addition to considering wave heights and relative direction, our novel modeling approach allows for evaluating also the impact of wave peak periods to the specific fuel consumption. The impact from waves of a certain height will significantly vary with wavelengths: Long waves (with relatively high peak periods) often occur in the aftermath of storms and periods with strong winds, and these waves contain less energy (and hence induce less added resistance) than shorter and steeper waves with short peak periods. As shown in Fig. 12 in Appendix A, waves at a certain wave height can occur with large spans in peak periods (T_p values), typically ranging from about seven seconds and up to 12 s for the most frequent wave conditions. In Fig. 7(a), the distance-specific fuel consumption is illustrated for four different wave states, each with a significant wave height of 3.5 meters and peak periods spanning from eight to 17 s. As seen, longer periods seem to yield a lower impact of the vessels and hence give a lower fuel consumption. At the same time, it is important to note that even shorter wave periods would reduce the fuel consumption. The highest consumption rate occurs for waves with a peak period $T_p = 8$, as seen in Fig. 7(b) where a constant sailing speed of 10 knots is assumed. Using the linear dispersion relation for waves on deep water, wavelengths can be approximated as $\lambda = \frac{g}{2\Pi} T_p^2$, which yields wavelengths of approximately 100 m. PSVs usually have a length of around 90 m, and when the length of the waves and the vessel length are fairly equal, the largest motions and hence added wave resistance are induced.

4.3. A framework for comparing different weather impact models

When performing speed optimization on the routing of PSVs operating in the North Sea, two existing approaches for calculating the fuel consumption have been applied in previously conducted research in addition to the novel approach we introduce in this paper:

1. Speed optimization with no considerations of the weather impact, referred to in the following as the *NoImp* approach. Here, only a single fuel consumption curve corresponding to the "calm water" sea state in Fig. 5(b) is applied for all sailing legs in any weather conditions.
2. Assuming wave height to be the single parameter affecting the operation of the PSVs, where a fixed speed loss is induced when wave heights are within certain discrete intervals. The magnitudes of these speed losses are based on empirical observations as presented in Table 1, and this approach is referred to as the *fixed speed loss* approach, *FSL*. Fuel consumption curves for the set of discrete sea states used in our experiments are shown in Fig. 5(b).
3. Lastly, we introduce in this paper the *HiFid* approach, where a high-fidelity numerical model is used to more precisely evaluate weather impact to the operability of PSVs. Weather conditions are described in three dimensions, namely wave height, wave period and wave direction relative to the heading of the vessels.

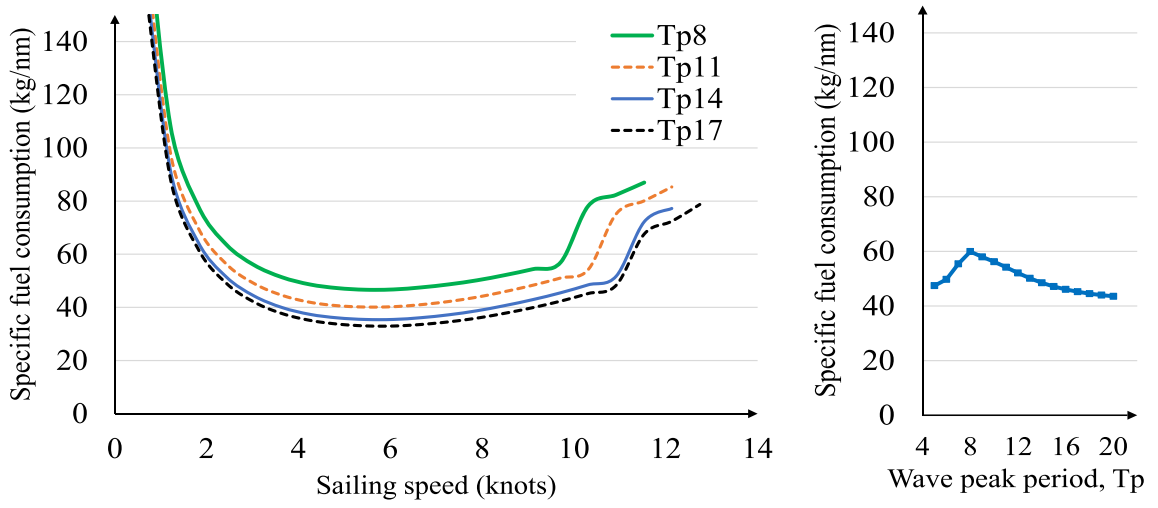

(a) Distance-specific fuel consumption rates as a function of sailing speed, for a set of different wave peak periods.

(b) Consumption as a function of wave period (speed $v = 10$ knots).

Fig. 7. Impact of the wave peak period (in seconds), T_p, to the distance-specific fuel consumption of the PSVs under consideration. Here, waves of height 3.5 m are evaluated (assuming only head seas) for peak periods occurring in the North Sea to a various extent in accordance with Fig. 12 in Appendix A.

Table 2
An overview of speed optimization strategies applied in offshore logistics planning, highlighting how they differ on methods for calculating weather impact and model fidelity. H_s, T_p and *Dir* refers to wave height, period and relative direction, respectively. Both references for *FSL* base the impact calculations on the approach introduced by Halvorsen-Weare and Fagerholt (2011).

Modeling approach	Impact calculation	Model fidelity			Weather variations		Reference
		H_s	T_p	*Dir*	*Temporal*	*Spatial*	
NoImp	n.a.						Norlund and Gribkovskaia (2013)
FSL	Empirical	✓			✓		Ulsrud et al. (2022), Norlund and Gribkovskaia (2017)
HiFid	Numerical	✓	✓	✓	✓	✓	This paper

Comparing how a higher model fidelity level might affect speed strategies and represent a potential for fuel (and emission) reductions on given routes is the main scope of our computational study. An overview of the three approaches is given in Table 2, where it is highlighted how weather is modeled at a different fidelity level in the *FSL* and *HiFid* approaches. A selection of the existing literature within offshore logistics planning applying the three different strategies is included for reference.

5. Computational study: A case from the North Sea

In this section, we quantify the effects of implementing our high-fidelity (*HiFid*) approach to modeling the weather impact compared to the simpler approaches *FSL* and *NoImp*. Implementation details and parameter settings used to obtain numerical values are described in Section 5.1. The generation of representative test instances to imitate real-life offshore logistics in realistic weather conditions is presented in Section 5.2. In Section 5.3, we compare the estimated fuel consumption obtained with the different approaches, while we discuss how this may impact the routing decisions for offshore logistics planners in Section 5.4.

5.1. Implementation and parameter settings

We base our weather scenarios on a combination of historical observations and a "hindcast" for the weather conditions in the North Sea over a three year period (2010–2012), provided by the Norwegian Meteorological Institute. We use three characteristics to describe weather conditions, namely significant wave height, H_s, wave period, T_p, and the direction of waves relative to the vessel's heading. Hindcast values are specified for each point in a grid spanning from 58-62°N and 0.0–4.5°E, with a grid resolution of 0.5°. The locations of the offshore installations in this "weather grid" are shown in Appendix B. Time is discretized at intervals of 15 min, in accordance with the approach presented by Ulsrud et al. (2022).

Model resolution settings and calculations of fuel consumption

Calculation of the weather impact to the PSVs in operation is provided by a hydrodynamic ship model as described in Section 4.2. While numerical results for the weather impact on ships in principle can be calculated for all different sea states using such models, there still is a need for a trade-off between high accuracy and fine resolution of the sea states on one hand, and more computational

Table 3
An overview of the selected parameter resolution for establishing the high-fidelity weather impact model.

Weather parameter	Min value	Max value	Increment
Significant wave height, H_s (m)	0.5	14	0.5
Wave period, T_p (s)	1	22	1.0
Wave direction relative to ship heading (°)	0	180	15

effort and solution time needed to calculate the weather impacts on the other. The selected sea state resolution presented in Table 3 has been deemed reasonable for the assessment of ship-weather impact calculations, while keeping the number of discrete sea states to represent real weather at a moderate level.

We see from Table 3 that direction of waves relative to the ship heading is placed in one out of a total of 12 intervals ranging from 0 to 180°. In other words, we assume a symmetric impact of the waves to the ship's performance, i.e., that waves approaching from the port and starboard side at the same angle have the same impact on a vessel. For each heading category, a total of 594 different discrete sea states can be defined with 27 possible wave heights and 22 possible wave periods. Additionally, we include the sea state referred to as "calm weather", where both wave height (H_s) and wave period (T_p) have a value of zero.

As real weather conditions are retrieved from historical data as high-precision continuous values both in terms of wave heights, periods and wave direction, it is not possible to establish the fuel consumption curve for all sea states. Hence, we do a four-step linear interpolation to link model data to the real weather encountered by the vessels during sailing:

1. The relative direction of waves to the ship heading is calculated, and two "extreme values" (`HdgLow` and `HdgHigh`) are selected from the range of discrete directions given from Table 3 (e.g., 45° and 60°, respectively).
2. Any weather condition encountered by the vessels is described in terms of both significant wave height and wave peak period. If a sea state is given as $H_s = 3.1$ m and $T_p = 7.6$s, four "corner point" sea states are created, namely `HLowTLow`, `HLowTHigh`, `HHighTLow` and `HHighTHigh` and here given as $[3.0, 7]$, $[3.0, 8]$, $[3.5, 7]$ and $[3.5, 8]$, respectively.
3. For each "corner point" sea state, the weather impact is known in terms of overall power requirements for the vessel, namely `Preq`, for various sailing speeds. To find the weather impact of the present weather conditions, a double linear interpolation over both wave height and wave period is performed using the corner point values.
4. Finally, linear interpolation between the `Preq` values in each of the two relative heading extremes is performed to find the resulting energy consumption curve used to evaluate the fuel consumption (or CO_2 emissions) for the selected sailing speed.

Vessel-specific characteristics

We consider a type of PSVs representative for the operations in the North Sea, with a cargo capacity (for deck cargo) of 100 container units and a loading and unloading rate of 10 units per hour (in good weather), in accordance with the computational studies by Ulsrud et al. (2022).

Using the mathematical (cubic) expression for the propulsion power given in Fig. 4 and assuming a constant auxiliary power requirement of 500 kW, which is translated into a distance-specific energy consumption as a function of speed, we can establish the approximation for calm water energy consumption (given in kWh/nm) for our case study PSV as

$$P(v) = 2.6v^2 - 30.5v + 210.3, \quad v \in [6, 15]. \tag{9}$$

The expression is defined over the interval [6, 15] knots, which represent the speed range with a convex energy consumption curve used in the process of generating discrete arrival times to each installation. Weather conditions will affect this feasible sailing speed range, both by limiting the maximum sailing speed and by allowing lower sailing speeds to be selected.

5.2. Generation of test instances

Our test instances are represented as the combinations of particular PSV routes visiting a set of offshore installations and different time series of sampled historical weather observations for the area of interest in the North Sea. In a real planning setting, an updated weather forecast would be available for the next 2–3 days, sufficiently long to complete the planned routes and visiting all offshore installations to meet their demands. It is worth noting that we treat the weather data to be deterministic, i.e., that we have a perfect forecast with no uncertainties associated with the forecasted weather conditions over the planning horizon of (maximum) 72 h. This is a reasonable assumption, given that the weather forecasts usually are quite accurate for the next 2–3 days.

We consider a set of 25 PSV routes obtained from the optimal solutions to the supply vessel routing problem described by Ulsrud et al. (2022). Key characteristics of these routes are summarized in Table 4. To each route, the maximum allowed duration (T^{MAX}) is calculated by assuming a fixed, fuel-efficient speed (10 knots) for all sailing legs and assuming no increase of servicing time or consumption rates due to weather conditions. This represents the route duration one would use as the "upper duration limit" in a planning context with no weather considerations. Furthermore, we do not consider any closing hours in our experiments, as the large majority of the installations visited on the selected routes operate round the clock.

The two choices described above when generating the test instances affect the obtained results in different ways: A maximum duration on each route ensures a higher average sailing speed closer to the design speed for the PSVs used as the basis for manual planning in the current practice, and hence makes results more valuable for the logistics planners in the industry. At the same time,

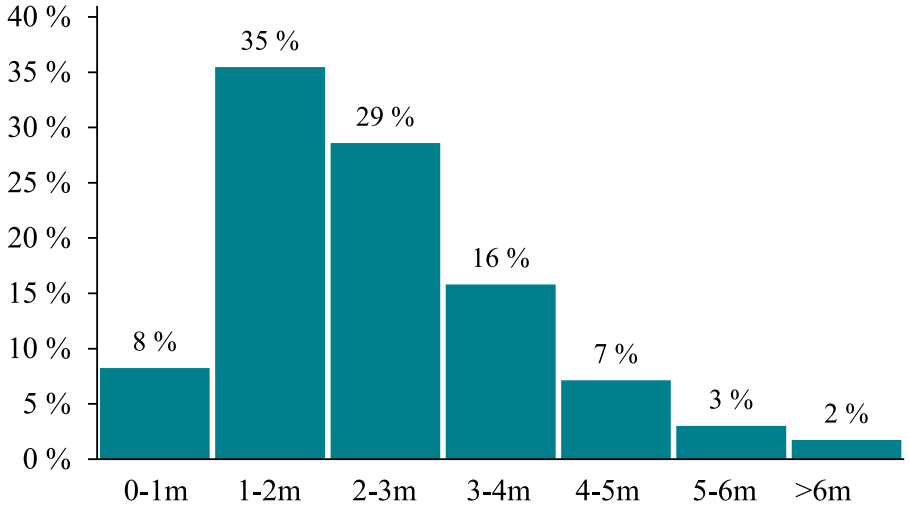

Fig. 8. Historical distribution of significant wave heights in the North Sea region, given as the relative share of the three years sample period (2010–2012) where different heights occur.

Table 4
Key characteristics of the PSV route categories, sorted by the number of sailing legs.

Route category	4 legs	6 legs	8 legs	10 legs
Number of routes	6	6	10	3
Avg. route distance (nm)	92.4	141.7	165.8	183.5

Table 5
Weather samples used for evaluation of the fuel consumption reduction potential from using a high-fidelity model for weather-dependent speed optimization. Every weather sample is a 72-hour time series starting at midnight on the specified starting date. WOW (Waiting On Weather) refers to the amount of time within the sample where wave heights exceed the safe limit (set to 4.5 m) for cargo lifting operations at the offshore installations.

WS	Starting date	Average H_s	Maximum H_s	WOW duration
1	05. aug. 2012	0.6 m	0.9 m	0 h
2	27. may 2012	0.9 m	2.2 m	0 h
3	13. jul. 2011	1.3 m	2.1 m	0 h
4	11. jun. 2010	1.9 m	4.0 m	0 h
5	15. jul. 2010	2.5 m	4.1 m	0 h
6	29. aug. 2012	2.7 m	5.0 m	5 h
7	18. sep. 2010	3.5 m	5.4 m	11 h
8	23. feb. 2012	3.8 m	6.7 m	7 h
9	22. feb. 2011	4.3 m	6.6 m	11 h
10	07. mar. 2012	4.7 m	7.2 m	16 h

it allows speed to be reduced to a minimum value in periods with harsh weather if this is found to give less fuel consumption overall. Conducting our experiments without constraints on opening hours at any installations yields a largest possible solution space where most speed alternatives are explored when evaluating the modeling approaches presented in Table 2.

There are numerous approaches to provide a set of representative weather conditions that PSVs will encounter during a normal year of operations in the North Sea. Fig. 8 displays the relative distribution of waves in discrete wave height intervals over the three year span of historical data. As can be seen, wave heights stay below five meters approximately 95% of the time. Based on the distribution of historical weather conditions, we consider weather samples with average wave heights covering the first five discrete intervals from Fig. 8. We further require from the samples that the maximum wave height during the sample period of 48 h is at least 50% higher than the average H_s. Finally, we pick the two samples within each wave category with the smallest and largest variability in observed wave heights over the sample period. The resulting ten *weather samples* with some key characteristics are given in Table 5.

5.3. Potential for reducing fuel consumption using the HiFid approach

We here compare the two speed optimization strategies *HiFid* and *FSL* in order to quantify the potential for fuel savings and hence emission reductions on PSV routes, through the use of the high-fidelity numerical model for calculating the weather impact.

Establishing performance measures for comparing modeling approaches

For a more realistic comparison of the two approaches, we introduce the notation *FSL-R* to represent the *realized* fuel consumption (or emissions) on the route using the *FSL* approach. To calculate the realized consumption on a route, we first fix on every sailing leg the speed decisions from the schedule that is obtained by applying the *FSL* approach, and then solve the speed optimization problem using a time–space diagram with only one sailing option between each sailing leg. The new *HiFid*-approach for a precise calculation of weather impact is then used to obtain the "true" fuel consumption for each leg on the route based on these speed decisions. In other words, we assume the numerical model used in the *HiFid* approach to represent (close to) the true weather impact on the vessel when performing the route using speed decisions from the *FSL* approach. To summarize, *FSL* and *FSL-R* yield the same speed selections on a route, but the former is obtained from a speed optimization *planning*, while the latter is a *realization* of these decisions with no flexibility or possibilities of adjusting the speed selections.

The overall route consumption for the *HiFid*, *FSL* and *FSL-R* approaches is then reported as E^{HF}, E^{FSL} and $\hat{E}^{FSL}$, respectively. These values contain the sum of fuel consumption from both sailing and idling (during servicing) at the installations. However, it should be noted that the different weather impact models in this paper only consider calculations of consumption during transit legs between the installations. For computing the fuel consumption from idling, we use for all speed optimization approaches a simplified method where a fix increase of required time and consumption (compared to the calm water reference values) is induced based on discrete weather states as shown in Table 1.

Based on the three consumption measures described above, we can further define two key performance indicators used to evaluate the two speed optimization strategies *HiFid* and *FSL*:

1. The *improvement* potential, abbreviated *IMP*, is the relative difference between the realized *FSL* solution (i.e., *FSL-R*) and the obtained *HiFid* solution and is computed as

$$IMP = \frac{\hat{E}^{FSL} - E^{HF}}{\hat{E}^{FSL}}. \tag{10}$$

   Due to the definition of the consumption measures and the way realized consumption is calculated, the *HiFid* solution will always yield a lower (or equal) consumption as the *FSL-R* solution and hence, *IMP* can only take non-negative values.
2. The relative error, *RE*, is defined as the relative miscalculation error of the initial speed strategy obtained by the *FSL* approach, when realizing the schedule and calculating the true consumption based on the high-fidelity weather impact model. We compute *RE* as

$$RE = \frac{|\hat{E}^{FSL} - E^{FSL}|}{E^{FSL}}. \tag{11}$$

   Positive values of *RE* mean that the true (realized) fuel consumption on a route is higher than planned by the *FSL* approach and represent an additional consumption that should be accounted for. On the other hand, negative values of *RE* mean that we have overestimated the true consumption for a given speed selection strategy on a route. However, this is not necessarily beneficial when also performing routing of vessels, as it might exist other routing alternatives that could be even more effective with a lower overall fuel consumption. In order to quantify the overall miscalculation better without cancellation effects from these two cases, we therefore report the absolute value for the relative errors.

Assessing the fuel reduction potential from the hifid approach

We evaluate the two performance indicators for the entire set of 25 routes in all 10 weather samples. The resulting improvement potentials and relative errors are given at an aggregated level in Table 6. Due to the characteristics of the selected weather samples, some routes could not be completed within the maximum duration for the route, T^{MAX}. For these instances, we have allowed a small extension of the maximum duration, sufficiently large to allow the routes to be performed at a *planning* level (i.e., to obtain a solution both for the *HiFid* and *FSL* approach). The number of routes where the duration has been extended is reported as n^{EXT}. Furthermore, it was observed that some of the speed decisions from the *FSL* approach were not possible to realize, meaning that a feasible solution for the *FSL-R* approach could not be obtained for certain routes. In other words, we find that the *FSL* approach creates less robust schedules than the *HiFid* approach as they cannot be realized in the actual weather conditions in certain instances. Thus, we disregard these results from the calculations of the average values of *IMP* and *RE* reported in Table 6, and the numbers of remaining feasible routes for each route category are given as n^F. We observe that the *FSL* approach fails to create feasible schedules more frequently in harsher weather and/or for longer routes.

As further observed from the results in Table 6, the largest emission reduction potentials (*IMP* values) are obtained in the harshest weather conditions, namely WS5 to WS10. A further review of the results reveals that savings are also highly route-specific. The average fuel consumption and emission reduction potential across all routes and weather scenarios (those where solutions can be obtained using both speed optimization strategies) is found to be 4.5%. At the same time, it can be observed that an average emission reduction potential (over all routes within a route category) of more than 2.0% is observed in 55% (22 out of 40) of the route category and weather sample combinations. In general, the improvement potential seems to increase with worsening weather (higher weather sample (WS) index values). Furthermore, the *RE* columns in Table 6 show that there are substantial miscalculation errors from using the *FSL* approach for all route categories and all weather samples. The average miscalculation errors span from 5.2 to 10.2% for the different route categories. A closer analysis of the reported results reveals two main reasons for these errors:

Table 6
Comparison of the *HiFid* and *FSL* speed optimization strategies, in terms of improvement potential in percent (*IMP*) using *HiFid*, and the relative miscalculation errors in percent (*RE*) using the *FSL* approach. The number of routes where no schedules could be obtained without extending the initial maximum duration is reported as n^{EXT}. Routes where the *FSL* approach could not be realized are disregarded from the comparison, and the number of feasible instances used to create the averaged values is counted as n^F.

Route cat.	4 legs				6 legs				8 legs				10 legs			
No. of routes	6				6				10				3			
WS	*IMP*	*RE*	n^{EXT}	n^F	*IMP*	*RE*	n^{EXT}	n^F	*IMP*	*RE*	n^{EXT}	n^F	*IMP*	*RE*	n^{EXT}	n^F
1	1.0	2.7	0	6	0.8	4.6	0	6	0.1	3.7	0	10	0.3	5.5	0	3
2	0.1	2.3	0	6	1.1	5.3	0	6	0.4	4.2	0	10	0.4	4.7	0	3
3	0.2	8.3	0	6	0.5	5.3	0	6	0.2	4.1	0	10	0.6	6.3	0	3
4	0.6	2.3	0	6	1.3	5.5	0	6	1.5	8.3	0	10	0.5	12.5	0	3
5	1.6	4.2	0	6	3.0	5.2	0	6	5.1	5.3	1	9	4.4	7.1	0	3
6	2.7	5.2	0	6	5.3	4.8	1	6	1.8	5.8	1	6	5.7	2.9	0	3
7	10.0	17.2	6	6	24.6	16.3	6	6	11.5	9.1	9	9	14.2	13.7	3	3
8	4.5	8.1	1	6	5.8	10.9	5	6	10.2	11.2	6	6	21.3	5.1	1	1
9	10.8	11.4	1	6	10.4	9.5	5	6	12.3	7.5	7	7	9.4	4.7	1	1
10	10.2	40.5	6	6	7.6	19.1	5	5	9.8	32.0	6	6	8.6	2.3	2	2
Avg.	**4.2**	**10.2**			**5.9**	**8.3**			**3.9**	**5.2**			**4.2**	**5.8**		

Table 7
Selected sailing speeds (in knots) for each leg on a given six-legged route planned in weather sample WS8, for the two different speed optimization strategies *HiFid* and *FSL*. Bold values highlights the differences between the two strategies.

Approach	Leg 1	Leg 2	Leg 3	Leg 4	Leg 5	Leg 6	Total duration
HiFid	**9.8**	**11.0**	12.3	11.8	7.4	**12.0**	39 hrs
FSL	**12.8**	**14.4**	12.3	11.8	7.4	**11.0**	39 hrs

- First, neither wave direction nor wave period are considered in the *FSL*, and hence, the estimated forced speed loss is considered to be independent of where waves are coming from. As seen from Figs. 6 and 7(a), direction and period clearly influences the estimated speed losses for PSVs.
- Second, and perhaps more significant, the *FSL* approach does not consider spatial variations of the weather considerations (as indicated in Table 2). Instead, a fixed point in the middle of the region of interest is used as a reference for the weather forecast throughout the duration of a route, in accordance with the implementation by both Halvorsen-Weare and Fagerholt (2011) and Ulsrud et al. (2022).

To gain better insight in the different speed selection decisions made using the two compared planning strategies, Table 7 illustrates for a route with six sailing legs how the determined sailing speeds obtained for both the *HiFid* and *FSL* approach differ when the route is planned to be performed in weather sample WS8. In this example, different speed selections are observed for three legs on the route, but the total duration of the route remains unchanged. The *HiFid* approach yields a schedule where speed is reduced on the early stages of the route, and with a higher speed on the final leg compared to the solution obtained from the *FSL* approach. For this particular weather sample, wave conditions are considerably worse in the first part of the sample period, and the speed selection strategy obtained using *HiFid* hence allows for less fuel-consuming sailing for this part of the voyage.

The selection of sailing speeds obtained using the *HiFid* approach and presented in Table 7 yields an emission reduction potential of approximately 14% for WS8. Fig. 9 displays the relative share of sailing time spent in different wave heights and headings as a result of the speed selections obtained by applying the two different strategies. As can be observed, the reduced speeds on the first two legs using the *HiFid* approach (Fig. 9(a)), combined with a higher sailing speed for the final and longest leg, ensure that the vessel avoids sailing (and also servicing installations) in the harshest weather conditions. Significant fuel reductions are achieved even though a larger portion of the voyage is performed in head seas.

A special feature of the PSV routes found in offshore logistics compared to most other short sea shipping services, relates to the weather-dependent servicing at installations. Weather conditions affect both the servicing time and the fuel consumption rate when idling, and from our objective function (1), it is the *total* fuel consumption on a route that is minimized. This means that in some cases, the *HiFid* approach finds solutions where the *sailing* costs are higher, but with shorter servicing time in better weather conditions. Thus, the overall fuel consumption is still lower than the realized schedule obtained from the *FSL* approach. From a further review of our results, we find that on average approximately 60%–70% of the total fuel consumption stems from sailing and that this is to a large extent independent of the weather conditions. Relatively less time is spent on sailing in harsh weather conditions (as more time is spent on servicing), but at the same time, sailing takes place in worse weather yielding higher fuel consumption rates. As previously discussed in Section 5.2, speed decisions are also to some extent affected by the maximum duration imposed to each route. However, opposed to liner shipping services, we do not have a strict schedule to follow with time slots at the ports/installations, and hence there is more flexibility with regards to selecting sailing speeds individually for each leg.

To evaluate the extent of different speed selections at an aggregate level (i.e., for every route considered in every weather sample), we define the indicator l^{diff} as the average number of legs where the selection of sailing speed differs between the two strategies. In cases where all speed decisions are equal on every leg on a route scheduled for a given weather sample, we instead count this

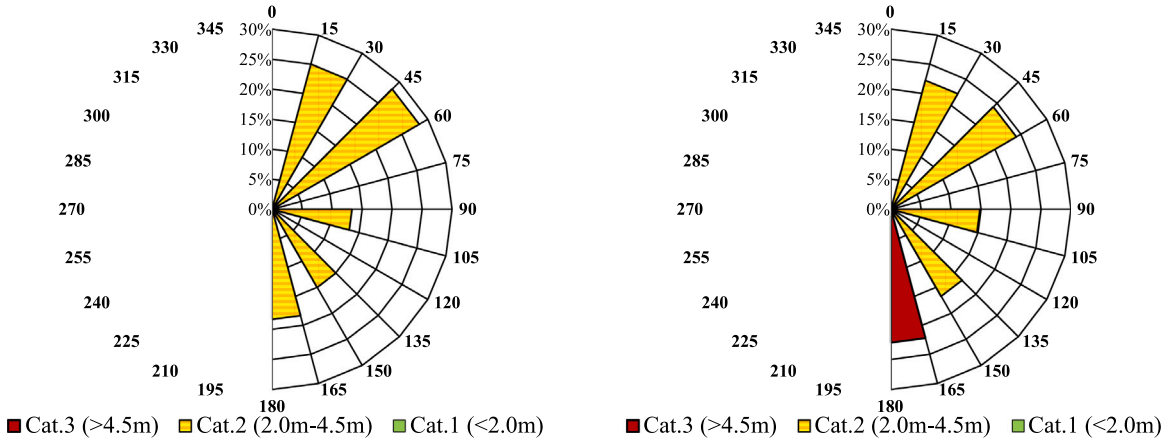

(a) *HiFid* approach

(b) *FSL* approach

Fig. 9. Distribution of sailing in different sea states for the *HiFid* approach (left) and the *FSL* approach (right), illustrated as the share of total sailing time on a six-legged route (in %) where the vessel experiences the different weather conditions in weather sample WS8.

Table 8
Comparison of speed optimization strategies on an aggregated level, i.e., for all routes scheduled in all weather samples. Note that the values for the l^{diff} indicator are presented as the average number of legs with different speed selections per route within the route category. s^{ID} represents the number of identical speed selections, within each route category and weather sample, i.e., where the speed decisions obtained by the two strategies are exactly the same for all legs on a route.

Route cat.	4 legs		6 legs		8 legs		10 legs	
No. of routes	6		6		10		3	
WS	l^{diff}	s^{ID}	l^{diff}	s^{ID}	l^{diff}	s^{ID}	l^{diff}	s^{ID}
1	0.7	3	0.7	2	0.9	5	0.3	2
2	0.3	5	1.7	1	1.3	4	1.0	0
3	1.0	3	1.0	2	1.1	3	2.0	1
4	0.3	4	1.2	0	2.3	3	1.3	0
5	0.8	3	1.5	1	2.9	0	2.7	0
6	1.2	2	1.7	0	2.1	1	4.7	0
7	2.2	0	4.3	0	4.3	0	6.7	0
8	1.7	0	3.0	0	4.0	0	6.0	0
9	1.5	0	3.2	0	4.5	0	7.7	0
10	2.2	0	3.7	0	4.4	0	5.0	0

as an *identical speed selection*, denoted s^{ID}. In Table 8, we report the results for all routes scheduled in all weather samples, and compare these two indicators on an aggregated level for each route category. We observe that the difference between the two speed optimization strategies increases with worsening weather (WS6 to WS10), through a larger average l^{diff} value and fewer (none) identical speed selections, S^{ID}.

Modifying the FSL approach to contain spatial weather variations

The *FSL* approach uses a weather forecast for a fixed geographical point in the North Sea, which affects the sign of the miscalculation errors reported in Table 6 in terms of absolute values. In cases of underestimation of the true consumption (negative *RE* values), weather might have been better at the selected reference location than the weather in the regions where the route is performed, and vice versa in the cases of overestimation of consumption (positive *RE* values). As illustrated in Fig. 10, observed wave heights in the area of interest in the North Sea varies greatly with location as well as time, which partially explains the magnitude of miscalculation errors.

An obvious adjustment to the *FSL* approach is therefore to update weather conditions at the same frequency and in the same way as for the *HiFid* approach, for a more realistic comparison of the two strategies. This way, the weather impact is evaluated at the beginning of every new sailing leg for both strategies, using the weather conditions at the most recently serviced installation as the current weather. This is a relatively straightforward implementation that does not affect the solution procedure or experimental setup. We refer to this approach as the *modified* fixed speed loss approach, *mFSL*, for which the results are presented in Table 9.

As we can observe, the overall average emission reduction potential (across all weather samples and route categories) by applying the *HiFid* approach is reduced to 0.9%, and only in 20% (8 out of 40) of the instances the high-fidelity model yields average fuel reductions of more than 2.0%. Furthermore, there is a very limited improvement potential for all routes in the samples of good weather, and in 12 out of 40 test instances, no differences in speed selection are observed at all for any of the routes within the

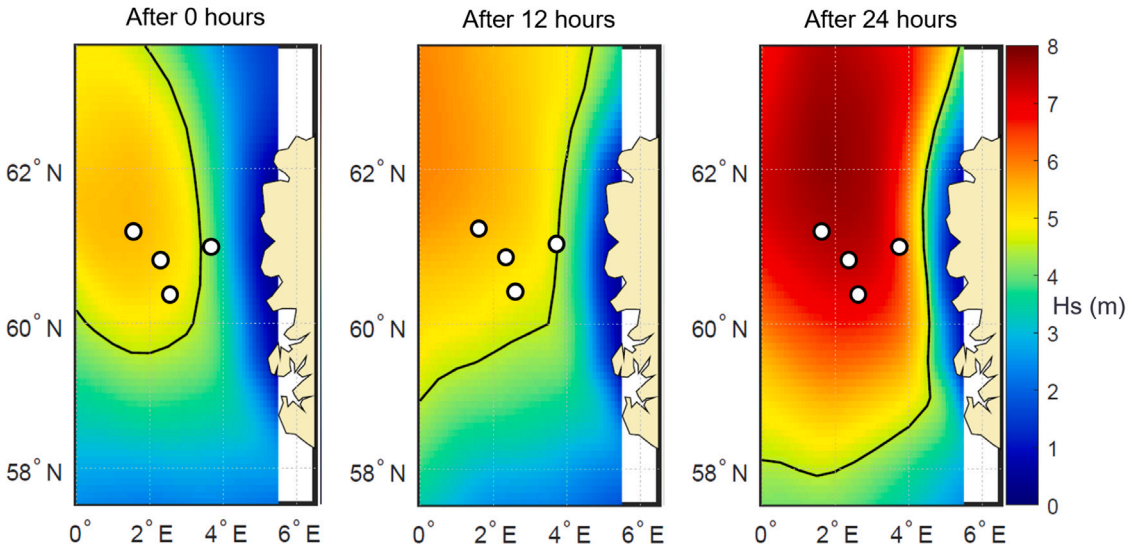

Fig. 10. The spatial and temporal variation of significant wave heights (H_s) in the North Sea over a 24-hours period representative for weather conditions in January, including the approximate location of some large clusters of offshore installations. The black, solid line indicates the wave limit ($H_s \leq 4.5$ m) for safe service at the installations.

Table 9
Comparison of the *HiFid* approach to a modified version of the *FSL* approach, *mFSL*, where also spatial variations of weather are accounted for. The two strategies are compared in terms of improvement potential (*IMP*) using *HiFid*, and the relative miscalculation errors (*RE*) using the *mFSL* approach. The number of routes where no schedules could be obtained without extending the initial maximum duration is reported as n^{EXT}. Routes were the *FSL* approach could not be realized are disregarded from the comparison, and the number of feasible instances used to create the averaged values is counted as n^F.

Route cat.	4 legs				6 legs				8 legs				10 legs			
No. of routes	6				6				10				3			
WS	*IMP*	*RE*	n^{EXT}	n^F	*IMP*	*RE*	n^{EXT}	n^F	*IMP*	*RE*	n^{EXT}	n^F	*IMP*	*RE*	n^{EXT}	n^F
1	0.0	2.1	0	6	0.0	3.8	0	6	0.0	3.6	0	10	0.1	5.1	0	3
2	0.0	2.2	0	6	0.0	4.8	0	6	0.1	4.1	0	10	0.0	5.8	0	3
3	0.0	5.3	0	6	0.0	5.0	0	6	0.0	4.0	0	10	0.0	6.3	0	3
4	0.0	1.7	0	6	0.1	4.1	0	6	0.7	6.6	0	10	2.3	10.7	0	3
5	0.0	5.3	0	6	0.6	3.1	0	6	2.4	4.8	1	9	2.6	5.4	0	3
6	0.1	7.3	0	6	0.0	4.3	1	6	0.7	3.8	1	7	4.3	3.1	0	3
7	0.9	6.6	6	6	0.2	6.3	6	6	0.3	6.0	9	9	0.0	4.4	3	3
8	2.6	13.3	5	6	7.7	8.4	5	6	0.7	4.0	10	10	0.2	1.1	2	2
9	1.8	7.4	5	6	2.7	7.7	5	6	2.4	3.3	9	9	0.1	2.2	1	1
10	1.0	4.8	6	6	0.4	3.2	5	5	0.2	2.7	9	9	0.1	1.8	3	3
Avg.	**0.6**	**5.6**			**1.2**	**5.0**			**0.7**	**2.6**			**1.0**	**4.4**		

route category. At the same time, significant reductions of the relative estimation errors are seen for all route categories and weather samples.

The *mFSL* approach also yields more robust schedules for routes planned in the worst weather conditions compared to the original *FSL* approach that has been applied in the existing literature on the field. This can be seen by comparing the number of feasible instances obtained when performing speed optimization with these two variants. We observe from Table 9 the increased value of n^F for the eight- and ten-legged routes in the harshest weather conditions, which strengthens the findings regarding *IMP* and *RE* values as more instances are included in the calculation of these averaged values than for the results using the *FSL* approach.

5.4. The effect of model resolution to offshore routing problems

This section contributes to answering the second research question stated in Section 1. In order to conclude on whether a more precise approach (such as the *HiFid*) can affect not only the speed selection on given routes, but also the optimal routing decisions themselves, we carry out a final experiment where we simply reverse the *direction* for the sampled set of PSV routes. As the *mFSL* approach proves to yield better results than the initial *FSL* approach, we here select *mFSL* as a benchmark for the *HiFid* approach.

For every of the 25 routes in every of the 10 weather samples, we calculate the fuel consumption for the *planned* schedule and obtain E^{HF} and E^{mFSL} as in Section 5.3, both for sailing the route in the *initial* direction and in the *reversed* direction. We then count by *nDiff* the number of instances where the two approaches identify different sailing directions as the least consuming sailing

Table 10
Impact of weather model fidelity on routing decisions: *nDiff* refers to the number of routes where the two model approaches *HiFid* and *mFSL* conclude differently on whether sailing the considered routes in the reverse direction (i.e., opposite of the initial route direction) yields a better solution or not.

Route cat.	4	6	8	10
No. of routes	6	6	10	3
WS	*nDiff*	*nDiff*	*nDiff*	*nDiff*
1	2	3	6	0
2	1	1	2	0
3	2	3	2	2
4	1	1	2	2
5	2	1	1	0
6	4	2	2	0
7	1	0	0	2
8	3	3	1	0
9	2	1	3	1
10	1	0	0	0

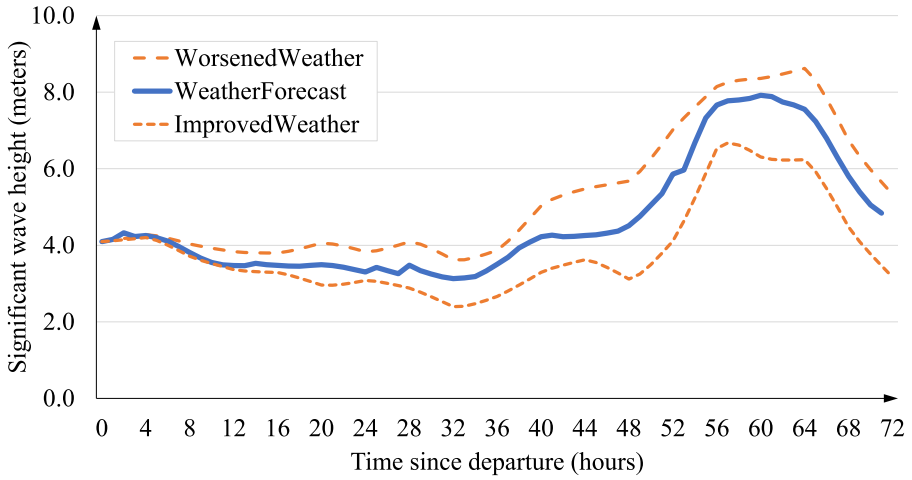

Fig. 11. Two generated scenarios illustrating the uncertainty in wave height development over time for weather sample 8 (WS8) presented in Table 5. Wave heights can be up to 30% higher (Worsened) or lower (Improved) than the forecasted value, and the forecasting error is increasing with time.

alternative. This performance measure is an indication of the effect on the routing decisions by the selection of a weather impact model, as sailing a route in two different directions also represents two different routing options.

As shown in Table 10, the two modeling approaches agree to a large extent (lower values of *nDiff* in worsening weather conditions and for longer routes), although no clear patterns can be observed. In cases where the two speed optimization strategies *HiFid* and *mFSL* conclude differently on the sailing direction for a route, the consequence of choosing the sub-optimal ("wrong") sailing direction (in terms of additional consumption) can be relatively large for both strategies (approximately 10% for WS7 to WS10). As for the initial *FSL* approach, it is important to note that the calculated consumption from using the *mFSL* approach, E^{mFSL}, represents the *expected* fuel consumption in either direction. The sailing direction found to be optimal using the *HiFid* approach will always represent the option yielding the lowest *realized* fuel consumption.

5.5. Addressing uncertainty in forecasted weather conditions

As stated in Section 5.2, we consider the weather forecasts in the North Sea to be sufficiently accurate (over the planning period of up to 72 h) to be treated as deterministic input. This assumption is mostly reasonable, but observations from operators in the North Sea suggest that the weather forecast is not always correct, both regarding the magnitude of wave heights and wind speeds, and also regarding at which point in time the forecasted weather conditions actually occurs. To investigate how the findings presented in this section can be affected by uncertainty in weather forecasts, we perform a simple analysis presented in the following.

According to Table 9, the largest emission reduction potential (largest *IMP* value) is for the routes with six legs in weather sample 8. Hence, we study the effects of weather uncertainty on these routes by creating a "wave height span" with two scenarios named *Improved Weather* and *Worsened Weather*, as illustrated in Fig. 11. In each of these two scenarios, we assume that the uncertainty increases with time and that the deviations from the forecasted wave heights reach 30% at the end of the planning horizon.

We evaluate the solutions to the speed optimization problem for each route using a similar calculation as presented in Section 5.3, i.e., using Eq. (10). For the two scenarios representing the forecast uncertainty, we first find the optimal schedule using the

Table 11
Additional realized fuel for routes in the category "6-legged routes" for weather sample 8. The table presents the calculated consumption when comparing the obtained solutions from the *HiFid* and *mFSL* approaches, respectively, to the obtained solutions generated when assuming perfect weather information for two scenarios. Tests are carried out for two test weather scenarios named *Worsened* and *Improved* weather.

Route no.	Improved weather		Worsened weather	
	HiFid-R	*mFSL-R*	*HiFid-R*	*mFSL-R*
Route 1	15.6%	28.2%	24.9%	33.8%
Route 2	3.2%	16.2%	12.0%	14.3%
Route 3	16.5%	30.0%	18.9%	20.0%
Route 4	33.1%	33.1%	24.0%	24.0%
Route 5	12.1%	23.1%	20.4%	22.9%
Route 6	6.5%	18.8%	42.9%	35.7%
Avg.	**14.5%**	**24.9%**	**23.9%**	**25.1%**

HiFid approach and assuming these weather forecasts to be known and deterministic. Thus, we find the theoretically lowest fuel consumption on any route given perfect weather information and denote this as the perfect information (PI) solution. Second, we *realize* the *HiFid* and *mFSL* solution found using the initial weather forecast in each of the two new scenarios. These realized costs are denoted *HiFid-R* and *mFSL-R*, respectively. Comparing these values to the *PI* solution gives us the relative value of perfect information. These results are summarized in Table 11.

Two observations can be made from the results in Table 11: First, we see that the *HiFid* approach in general performs better in uncertain weather conditions (both for improved and worsened weather) than the *mFSL* approach, as the additional cost of not having perfect weather information is lower for all routes except one (route 6). Second, we observe that the advantages of applying the *HiFid* approach are smaller when weather turns out to be worse than expected as the relative cost increase of the *HiFid-R* solutions are higher than for the corresponding *mFSL-R* solutions. From this, we can deduce a third finding: The emission reduction potential, presented as the *IMP* values in Table 6 and Table 9, is larger than reported in cases where weather turns out to be better than expected, and vice versa in worsened weather.

These results suggest that the proposed *HiFid* approach overall is more robust than the current approach using fixed speed losses to calculate weather impacts, meaning that speed decisions that are made based on the *HiFid* approach will create a schedule that performs better also when weather conditions turns out not to be as forecasted.

6. Concluding remarks

When performing operational planning within offshore logistics, involving the scheduling of platform supply vessels to offshore installations, weather conditions should be accounted for in order to obtain more robust schedules that can be performed also in harsh weather. However, most research in the field has been performed with a simplified approach to modeling the weather impact, and there is a lack of understanding regarding how the routing and scheduling strategies will be altered by accounting for weather in more detail during the operations planning.

With our approach based on numerical hydrodynamic models integrated in a speed optimization procedure, we find that the existing approach using fixed speed losses for discrete weather states, and not accounting for the direction or period of waves, yields significant miscalculations of the true (realized) fuel consumption for PSV routes. In other words, hydrodynamic considerations should be a part of the assessment when solving maritime scheduling problems in order to fully exploit the emissions reduction potential from weather routing.

In a real case of offshore logistics planning, routes for multiple vessels are determined simultaneously. Simple assessments of how the routing itself can be affected by the resolution level of the weather impact modeling reveal a potential for further increasing the benefits of weather-dependent routing with speed optimization compared to most current industry practices. A high-fidelity model allows for exploiting new and more robust schedules by selecting different sailing speeds for each leg, yielding a lower realized fuel consumption overall. These schedules are also found to perform better on average when considering uncertainty in the weather forecasts used for planning.

Our computational study is applied to a case within offshore logistics, but the same approach can be applied also to other shipping services where weather is assumed to impact the operability of vessels. It is reasonable to assume that the saving potential by accounting for direction-dependent weather impact becomes larger for sailing routes typically found in offshore logistics, with short legs and a relatively large share of a route spent on idling and servicing, and where weather conditions and the sailing direction on each leg change frequently. At the same time, there is a potential for reducing fuel consumption and emissions also for other short sea shipping services applying the high-fidelity approach to model weather impact. Time constraints related to tides or slot times (berth capacities) in ports can be handled directly in the model, although this will limit the flexibility in selecting sailing speeds for each leg and hence the potential for fuel savings. Furthermore, it could be considered to also include routing decisions in order to fully utilize the potential of the high-fidelity model presented in this paper. Our results suggest that making the correct routing decisions (e.g., selecting the least fuel-consuming direction for a route) will represent an even larger potential for emission reductions when combined with high-fidelity scheduling of the routes. On the other hand, the proposed model and solution approach in this paper will not be suitable for long-haul routes found in deep sea shipping, as uncertainty in weather forecasts and a challenge with

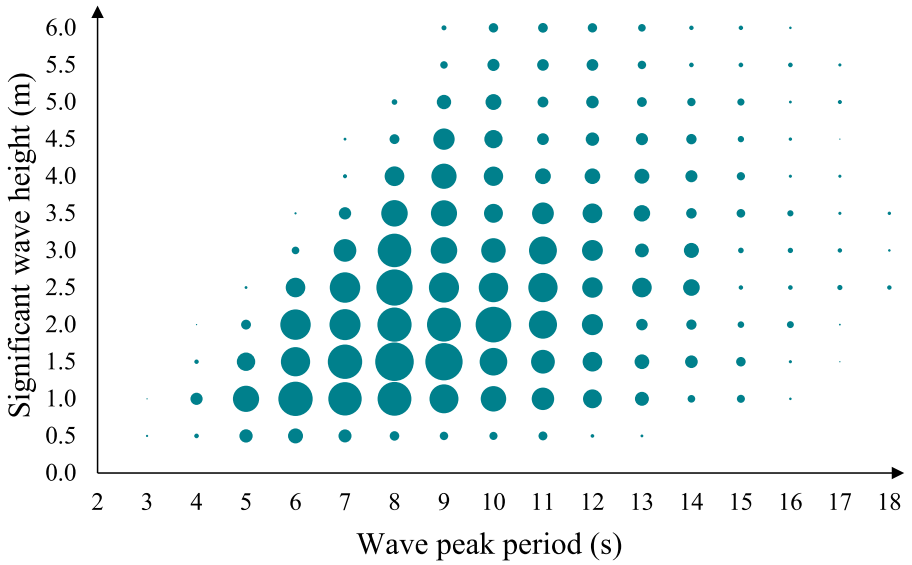

Fig. 12. Relative frequency of different sea states (combination of wave height and peak period) over the three years sample period (2010–2012). Larger circular dots represent a larger frequency of the given sea state, which is here discretized at the same resolution as the input parameters presented in Table 3 for the high fidelity weather impact model.

a computationally intensive solution procedure for long routes will require other modeling approaches in order to provide useful insights regarding weather-dependent routing and scheduling of vessels.

Our presented solution approach also has some limitations that should be addressed in further detail in future research. First, there is currently a lack of precise models for evaluating the weather impact to the operation of PSVs when in dynamic positioning mode (for idling and servicing), and consumption related to these activities can account for a large share of the overall route consumption. Second, in our reported results for speed decisions, we are assuming that the same speed should be maintained for the entire leg. This can be interpreted as the average sailing speed, but details on how to actually reach the next installation at the specified arrival time requires more attention. As weather changes rapidly in the North Sea, fixing the speed on entire sailing legs might restrict the model from finding the least fuel-consuming sailing strategies. To evaluate this effect on the overall consumption reduction potential on routes, we suggest studying a dynamic discretization factor and/or a splitting of sailing legs into shorter "sublegs", to create more flexibility in speed decisions along a route.

Declaration of competing interest

The authors declare that they have no known competing financial interests or personal relationships that could have appeared to influence the work reported in this paper.

Acknowledgments

The conducted work has been based on models developed by SINTEF and validated through Wei He in Equinor. We are grateful for the provided input data making it possible to conduct the described research at a high precision level and hence provide valuable insights to potential improvements that can be implemented by the logistics planners in a real-life setting. Furthermore, we would like to thank the industrial partners in the *LowEmission* research centre and the Research Council of Norway for financing this project.

Appendix A. Historical observations of wave conditions in the North Sea

See Fig. 12.

Appendix B. Offshore installations and weather grid

See Fig. 13.

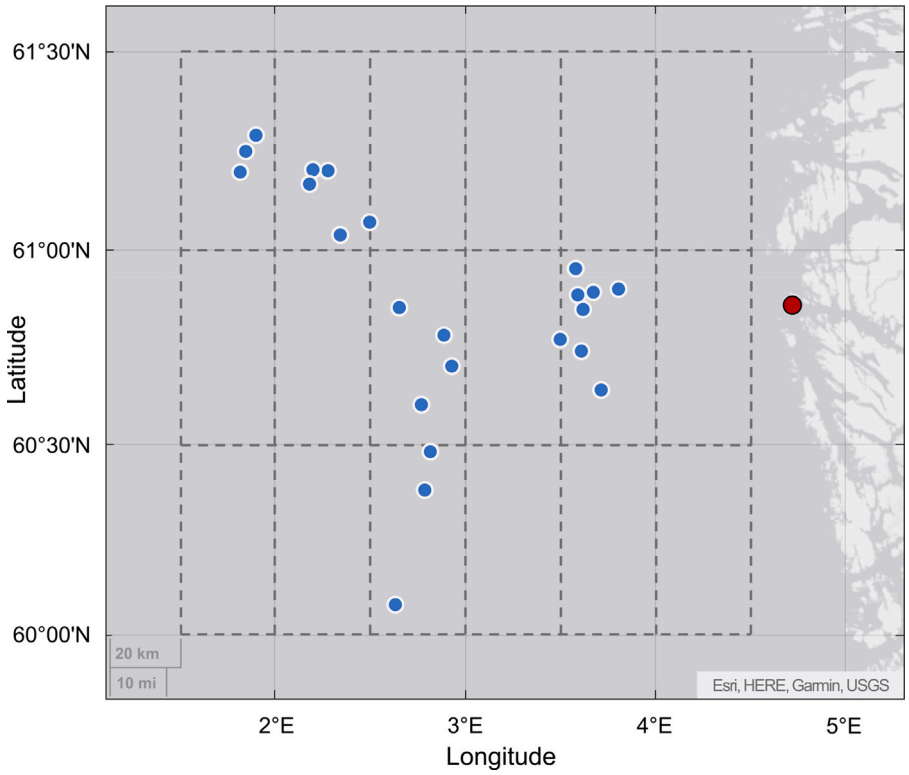

Fig. 13. Geographical location of the offshore installations visited on the set of sampled PSV routes in this study. The red dot represent the onshore supply base north of the city of Bergen, Western Norway. Dashed lines represent the weather grid for historical observations of wave conditions. (For interpretation of the references to color in this figure legend, the reader is referred to the web version of this article.)

References

Adland, R., Cariou, P., Wolff, F.-C., 2020. Optimal ship speed and the cubic law revisited: Empirical evidence from an oil tanker fleet. Transp. Res. E 140, 101972.
Brix, J., 1987. Manoeuvring technical manual. Schiff Und Hafen 36 (5).
Christiansen, M., Fagerholt, K., Nygreen, B., Ronen, D., 2013. Ship routing and scheduling in the new millennium. European J. Oper. Res. 228 (3), 467–483.
Cuesta, E.F., Andersson, H., Fagerholt, K., Laporte, G., 2017. Vessel routing with pickups and deliveries: an application to the supply of offshore oil platforms. Comput. Oper. Res. 79, 140–147.
Dickson, T., Farr, H., Sear, D., Blake, J.I., 2019. Uncertainty in marine weather routing. Appl. Ocean Res. 88, 138–146.
Du, W., Li, Y., Zhang, G., Wang, C., Zhu, B., Qiao, J., 2022. Ship weather routing optimization based on improved fractional order particle swarm optimization. Ocean Eng. 248, 110680.
Eide, L., Årdal, G.C.H., Evsikova, N., Hvattum, L.M., Urrutia, S., 2020. Load-dependent speed optimization in maritime inventory routing. Comput. Oper. Res. 123, 105051.
Fagerholt, K., 2001. Ship scheduling with soft time windows: An optimisation based approach. European J. Oper. Res. 131 (3), 559–571.
Fagerholt, K., Laporte, G., Norstad, I., 2010. Reducing fuel emissions by optimizing speed on shipping routes. J. Oper. Res. Soc. 61 (3), 523–529.
Grifoll, M., Borén, C., Castells-Sanabra, M., 2022. A comprehensive ship weather routing system using CMEMS products and A* algorithm. Ocean Eng. 255, 111427.
Grifoll, M., Martínez de Osés, F.X., Castells, M., 2018. Potential economic benefits of using a weather ship routing system at short sea shipping. WMU J. Maritime Affairs 17, 195–211.
Halvorsen-Weare, E.E., Fagerholt, K., 2011. Robust supply vessel planning. In: International Conference on Network Optimization. Springer, pp. 559–573.
Halvorsen-Weare, E.E., Fagerholt, K., Nonås, L.M., Asbjørnslett, B.E., 2012. Optimal fleet composition and periodic routing of offshore supply vessels. European J. Oper. Res. 223 (2), 508–517.
James, R.W., 1957. Application of Wave Forecasts To Marine Navigation. New York University.
Kepaptsoglou, K., Fountas, G., Karlaftis, M.G., 2015. Weather impact on containership routing in closed seas: A chance-constraint optimization approach. Transp. Res. C 55, 139–155.
Kim, M., Hizir, O., Turan, O., Day, S., Incecik, A., 2017. Estimation of added resistance and ship speed loss in a seaway. Ocean Eng. 141, 465–476.
Kisialiou, Y., Gribkovskaia, I., Laporte, G., 2018. The periodic supply vessel planning problem with flexible departure times and coupled vessels. Comput. Oper. Res. 94, 52–64.
Li, X., Sun, B., Guo, C., Du, W., Li, Y., 2020. Speed optimization of a container ship on a given route considering voluntary speed loss and emissions. Appl. Ocean Res. 94, 101995.
Mason, J., Larkin, A., Gallego-Schmid, A., 2023. Mitigating stochastic uncertainty from weather routing for ships with wind propulsion. Ocean Eng. 281, 114674.
Norlund, E.K., Gribkovskaia, I., 2013. Reducing emissions through speed optimization in supply vessel operations. Transp. Res. D 23, 105–113.
Norlund, E.K., Gribkovskaia, I., 2017. Environmental performance of speed optimization strategies in offshore supply vessel planning under weather uncertainty. Transp. Res. D 57, 10–22.

Norstad, I., Fagerholt, K., Laporte, G., 2011. Tramp ship routing and scheduling with speed optimization. Transp. Res. C 19 (5), 853–865.
Paixão, A., Marlow, P.B., 2002. Strengths and weaknesses of short sea shipping. Mar. Policy 26 (3), 167–178.
Psaraftis, H.N., 2019. Speed optimization vs speed reduction: The choice between speed limits and a bunker levy. Sustainability 11 (8), 2249.
Psaraftis, H.N., Kontovas, C.A., 2013. Speed models for energy-efficient maritime transportation: A taxonomy and survey. Transp. Res. C 26, 331–351.
Salvesen, N., Tuck, E., Faltinsen, O., 1970. Ship Motions and Sea Loads. SNAME, pp. 119–137.
Sen, D., Padhy, C.P., 2015. An approach for development of a ship routing algorithm for application in the North Indian ocean region. Appl. Ocean Res. 50, 173–191.
Shyshou, A., Gribkovskaia, I., Laporte, G., Fagerholt, K., 2012. A large neighbourhood search heuristic for a periodic supply vessel planning problem arising in offshore oil and gas operations. INFOR: Inf. Syst. Oper. Res. 50 (4), 195–204.
Simonsen, M.H., Larsson, E., Mao, W., Ringsberg, J.W., 2015. State-of-the-art within ship weather routing. In: International Conference on Offshore Mechanics and Arctic Engineering, vol. 56499. American Society of Mechanical Engineers, V003T02A053.
SINTEF, 2023. ShipX software. URL https://www.sintef.no/en/software/shipx/.
Ulsrud, K.P., Vandvik, A.H., Ormevik, A.B., Fagerholt, K., Meisel, F., 2022. A time-dependent vessel routing problem with speed optimization. European J. Oper. Res. 303 (2), 891–907.
Walther, L., Rizvanolli, A., Wendebourg, M., Jahn, C., 2016. Modeling and optimization algorithms in ship weather routing. Int. J. E-Navigation and Maritime Econ. 4, 31–45.
Yang, L., Chen, G., Zhao, J., Rytter, N.G.M., 2020. Ship speed optimization considering ocean currents to enhance environmental sustainability in maritime shipping. Sustainability 12 (9), 3649.
Zhang, G., Wang, H., Zhao, W., Guan, Z., Li, P., 2021. Application of improved multi-objective ant colony optimization algorithm in ship weather routing. J. Ocean Univ. China 20, 45–55.
Zis, T.P., Psaraftis, H.N., Ding, L., 2020. Ship weather routing: A taxonomy and survey. Ocean Eng. 213, 107697.